Supersonic Gas-Jet Characterization with Interferometry and Thomson Scattering on the OMEGA Laser System

Introduction

The generation of long, uniform plasmas is important to many disciplines in the laser–plasma interaction field. These plasmas are used in the study of laser–plasma instabilities relevant to inertial confinement fusion (ICF)[1] and the development of compact particle acceleration methods such as wakefield acceleration.[2] Supersonic gas-jet targets provide several advantages over comparable targets. Supersonic gas jets have excellent density profiles with steep gradients at the edges and consistent uniform densities in the central regions. This density profile is important for applications where propagation distance through the gas or plasma medium must be minimized before the laser beam reaches the experimental volume.

A wide range of plasma density regimes become accessible by modifying the backing pressure in the jet reservoir. The nozzle geometry can be modified to provide shaping and tuning of the gas-jet profile to experimental requirements. These features make the gas jet a versatile target. Other comparable targets, such as gas bags, rely on a solid-density envelope to maintain pressure prior to the experiment, but this outer skin generates blast waves with peak densities significantly greater than the central plateau density.[3]

The gas-jet system on the OMEGA Laser System[4] shown in Fig. 154.29 is a self-contained unit that was deployed from a TIM (ten-inch manipulator). The gas-jet system uses a fast opening and closing electromagnetically controlled valve fitted with a supersonic nozzle.[5] The valve is designed for use at high pressure (~1000 psi) to make possible the generation of high-density jets. The gas supply system enables the use of a wide variety of gases and allows rapid reconfiguration between different experimental demands.

To operate at high pressures, a strong return spring and a high-current electromagnet with a high-energy capacitor bank are used in the valve-control system. The high-energy capacitor bank is housed in a sealed atmospheric bubble at the rear of the apparatus. Together these components make it possible for the valve to be opened in ~100 μs and closed in <500 μs. The rapid opening and closing of this gas jet reduces the contamination of the high-vacuum environment that is required to protect sensitive diagnostic electronics prone to dielectric breakdown.

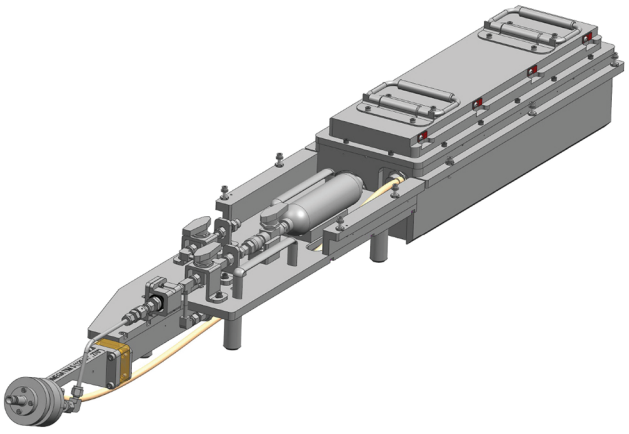

E27023JR

Figure 154.29
A complete engineering drawing of the gas-jet system. The control electronics are housed in the sealed box at the back of the system. The supply cylinder and a system of valves and plumbing feed the gas-jet reservoir. Inside the gas-jet body, an electromagnetic coil actuates a valve to allow the target gas to flow through the supersonic nozzle.

The ability to generate a consistent and well-characterized plasma is important for future laser-plasma experiments. A time-resolved Mach–Zehnder interferometer was used to measure the neutral density throughout the jet. The OMEGA Laser System was used along with the Thomson-scattering system (TSS) diagnostic[6] to measure plasma characteristics. These experimental parameters are then compared to an analytic gas-jet model.

Supersonic Nozzles

A supersonic gas jet generates a flow of gas that is moving with a velocity greater than the local sound speed. The density profile can be predicted using an analytic model of the behavior of a compressible ideal gas moving through the supersonic converging–diverging nozzle geometry.[7] Figure 154.30 shows an example of the converging–diverging supersonic nozzle

design. In this type of nozzle, the flow will accelerate until it reaches the speed of sound:

$$c_s = \sqrt{\frac{\gamma RT}{\mathcal{M}}}, \tag{1}$$

where γ is the adiabatic index, R is the molar gas constant, T is the temperature, and $\mathcal{M}$ is the molar mass. The flow velocity will be equal to the speed of sound at the throat of the nozzle, which is the point at which the cross-sectional area is smallest.

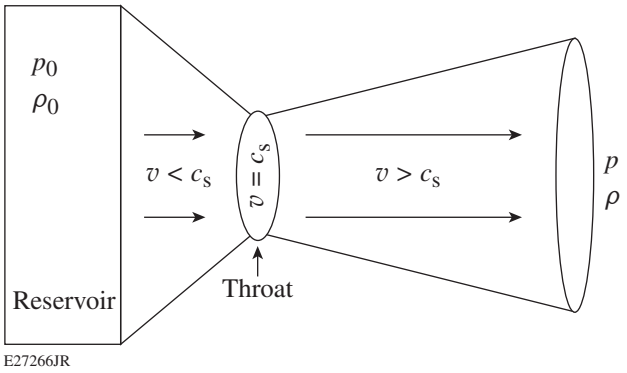

Figure 154.30
A sketch of a converging–diverging nozzle. In the converging section of the nozzle, the flow's velocity is below the speed of sound. The flow velocity will reach the speed of sound and then continue to accelerate past the throat of the nozzle into the diverging section.

As the gas moves from the throat, the gas undergoes isentropic adiabatic expansion in the diverging section of the nozzle, where it accelerates to supersonic velocities. This expansion is characterized by energy conservation,

$$C_p T_0 = \frac{v^2}{2} + C_p T, \tag{2}$$

where C_p is the specific heat of the gas at constant pressure and v is the velocity of the gas. The subscript "0" refers to conditions in the reservoir, while parameters without a subscript refer to conditions at the nozzle exit. Using this conservation equation, one can solve for all thermodynamic properties of the gas flow at all points along the nozzle. In these thermodynamic relations, the most-convenient variable for determining flow properties is the Mach number $\mathrm{M} = v/c_s$, which characterizes the flow velocity as a ratio to the sound speed. Using conservation of energy and solving in terms of the adiabatic index γ and Mach number M,

$$\frac{A}{A_*} = \frac{1}{\mathrm{M}}\left[\frac{2+(\gamma-1)\mathrm{M}^2}{\gamma+1}\right]^{\frac{\gamma+1}{2(\gamma-1)}}, \tag{3}$$

$$\frac{\rho_0}{\rho} = \left(1+\frac{\gamma-1}{2}\mathrm{M}^2\right)^{\frac{1}{\gamma-1}}. \tag{4}$$

Here, ρ_0 is the density in the reservoir, ρ is the density at the nozzle exit, A is the nozzle exit area, and A_* is the nozzle area at the throat. Assuming that gas parameters change smoothly along the entire length of the nozzle, Eq. (4) shows that the density ratio depends only on the Mach number and the adiabatic index of the target gas.

After the gas leaves the nozzle exit, a lineout of the gas density will have a flattop profile with a diameter equal to the nozzle exit diameter and the peak density defined by Eq. (4). Farther away from the nozzle, edges of the profile will be more gradual and expand at an angle approximately equal to 1/M. The full width at half maximum of the gas density can be estimated by

$$D = D_{\mathrm{exit}} + 2\frac{L}{\mathrm{M}}, \tag{5}$$

where D is the plume diameter, D_{exit} is the nozzle exit diameter, and L is the distance from the exit of the nozzle along the nozzle's axis of symmetry. Along with this geometric expansion, there is an accompanying decrease in density. The density in the center of the plume can be related back to the density at the nozzle exit:

$$\rho' = \rho\left(\frac{D_{\mathrm{exit}}}{D_{\mathrm{exit}} + 2\frac{L}{\mathrm{M}}}\right)^2. \tag{6}$$

The complete expression relating the density $\rho'(L)$ to the density in the reservoir ρ is

$$\rho' = \rho_0 \frac{1}{\left(1+\frac{\gamma-1}{2}\mathrm{M}^2\right)^{\frac{1}{\gamma-1}}}\left(\frac{D_{\mathrm{exit}}}{D_{\mathrm{exit}} + 2\frac{L}{\mathrm{M}}}\right)^2. \tag{7}$$

It is important to note that the Mach number of a particular nozzle is a function of the adiabatic index of the gas. For example, a Mach 3 nozzle designed for monatomic gases with $\gamma = 5/3$ will

be a Mach 2.6 nozzle when used with diatomic gases with γ = 7/5. Nozzle configurations for the OMEGA gas-jet system are defined by their monatomic Mach number and their exit diameter, which for a conical nozzle specifies all design parameters.

Nozzles used on the OMEGA gas-jet system are machined from 6061-T6 aluminum. The minimum throat diameter that can be manufactured is 0.25 mm, which is set by tooling aspect-ratio constraints. The maximum throat diameter is 3.6 mm, which is set by the size of the sealing surface that seats against the throat of the nozzle and creates the vacuum seal. These manufacturing constraints place limits on the Mach number and exit diameters of the gas-jet nozzles. Figure 154.31 shows the relationship between the exit diameter and the throat diameter for a range of Mach numbers along with the manufacturing limitations.

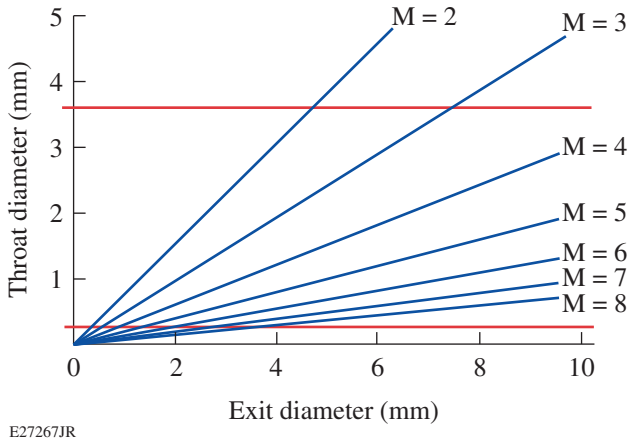

Figure 154.31
A plot of supersonic nozzle throat diameters versus exit diameters for various Mach numbers. Nozzles built for the OMEGA gas jet have a minimum throat diameter of 0.25 mm and a maximum throat diameter of 3.6 mm (shown as horizontal red lines). Mach numbers are calculated for gases with γ = 5/3.

Neutral Gas Density Measurement

The neutral density profile of the gas jet were measured using a Mach–Zehnder interferometer in a vacuum chamber separate from the OMEGA Laser System. In this setup, a 532-nm cw diode laser was expanded and collimated to an ~2-cm beam and split into two legs inside a vacuum chamber, where the probing leg was directed through the gas-jet plume. The image was captured using a PI-MAX3 camera, which uses a fast gate (~10 μs) to resolve the hydrodynamic evolution of the gas-jet plume as the valve opens and closes. The argon gas used in this experiment was chosen for its high index of refraction. To extract the density in the jet from the measured phase shift in the interference pattern, an Abel inversion was performed, which exploits the cylindrical symmetry of the gas plume to measure the density as a function of radius.[8] Figure 154.32(a) shows a measured interferogram and Fig. 154.32(b) the neutral density profile of the gas jet that was extracted from the phase shift using the Abel inversion.

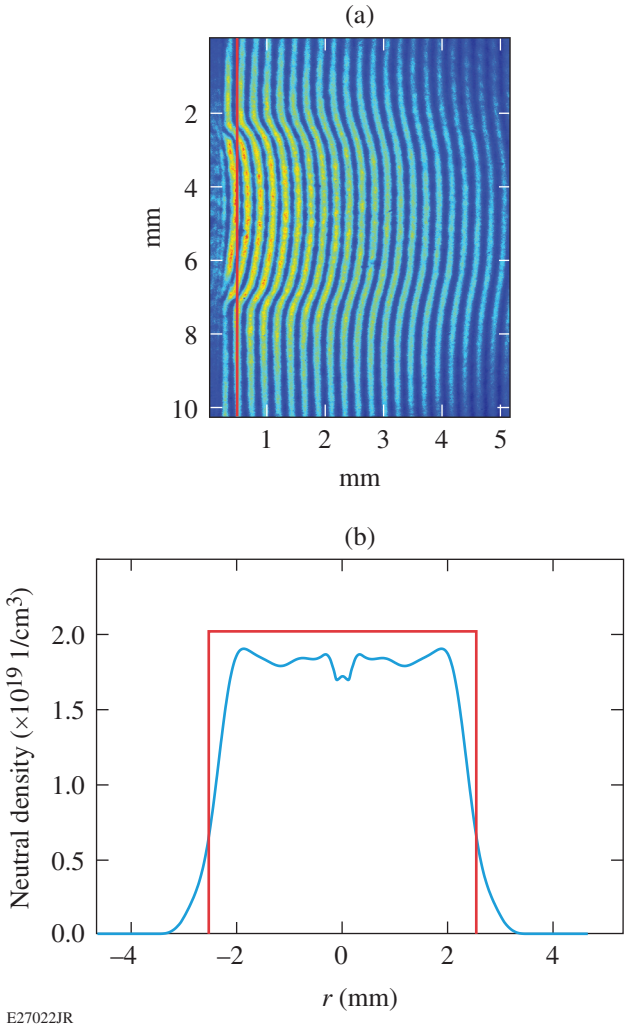

Figure 154.32
(a) An example image of the gas-jet interference pattern measured with the Mach–Zehnder interferometer and (b) a lineout of neutral density versus radius at 0.5 mm away from the nozzle in the gas plume. The flattopped density profile predicted by the analytic model is compared to the measured density profile.

Figure 154.33 shows the density in the gas-jet flow as a function of time. The valve opens in ~100 μs, reaches a steady-state density, and takes ~150 μs to close from a steady-state flow. The time that the gas jet spends in the steady-state flow

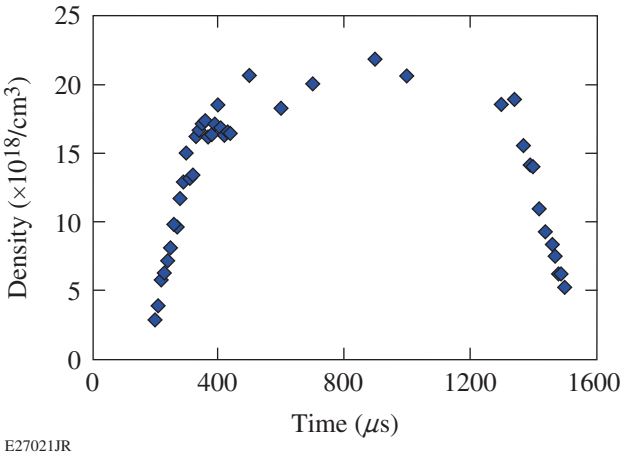

Figure 154.33
Density versus time was measured using a Mach–Zehnder interferometer and a 10-μs gated camera. The gas jet reaches steady state in 150 μs and then closes in a similar amount of time.

regime is dependent on the driving voltage and can range from ~500 μs to ~1 ms.

Plasma Density Measurement

Thomson scattering was used to characterize the conditions in the gas-jet plasma.[9] The OMEGA Thomson-scattering system uses one of the 60 OMEGA beams to provide a Thomson probe beam. The Thomson probe is frequency doubled to 526.5 nm in a 100-ps, square-shaped pulse with 20 J of energy in the *f*/6.7 beam.[10] For beam smoothing and optimal propagation through the plasma volume, a phase plate was used to produce a 200-μm-diam spot at the Thomson volume. Thomson-scattered light was collected along the probe's entire propagation distance through the plasma. An *f*/10 reflective Thomson-scattering collection system makes it possible to achromatically collect and transport the scattered light from the target plasma to a pair of spectrometers and cameras.[6]

To ionize the gas in order to produce a plasma, 11 frequency-tripled, 351-nm beams illuminated a 1-mm-diam spherical volume 1 mm from the end of the gas-jet nozzle. Each heater beam was a 1-ns-long, square-shaped pulse with 300 J per beam, making the total energy on target 3.3 kJ. The Thomson probe was delayed 250 ps compared to the heater pulses. The nozzle was a Mach 2.6 and the target gas was nitrogen.

The imaging Thomson-scattering spectra allow one to analyze the plasma conditions along the entire probe in an ~200-μm-wide channel. Figure 154.34 shows the EPW (electron plasma wave) feature along the Thomson-scattering probe.[11] The EPW feature was used to fit electron density by location of its peak and electron temperature by fitting its width. The flat region of the spectra between ±0.2 mm shows a nearly constant density plateau. The rapidly changing features on either side indicate a dropping density as a result of the rarefaction wave.

When the plasma is first formed, the pressure differential between the inside and outside of the plasma volume creates a rarefaction wave as the plasma expands into the surrounding space. This rarefaction wave is transmitted through the plasma at the ion sound speed $c_s = \sqrt{\gamma Z T_e / m_i}$. Using this velocity, the rarefaction wave takes ~1 ns to reach the center of the plasma volume, which is consistent with its location (200 μm) after 700 ps.

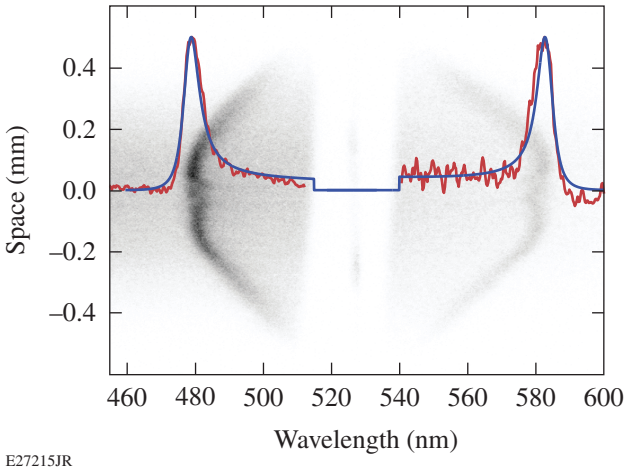

Figure 154.34
Imaging Thomson-scattering electron plasma wave feature of the gas-jet plasma. At the center of the plasma a lineout is taken and a fit is made using the Thomson-scattering form factor. The central portion of the spectrum is removed with a notch filter to remove light near the probe wavelength.

Figure 154.35 shows the density as a function of space through the plasma volume. The density in the central ~500 μm of the plasma is a constant plateau, similar to the measurements shown in Fig. 154.32. The analytic model does not include plasma hydrodynamics and therefore does not match the linear sloping sides of the density profile. The analytic model predicts a peak density ~30% higher than the peak density that is measured with Thomson scattering. In similar experiments this discrepancy between the analytic and experimental peak density was measured to be ~20% to 10%.

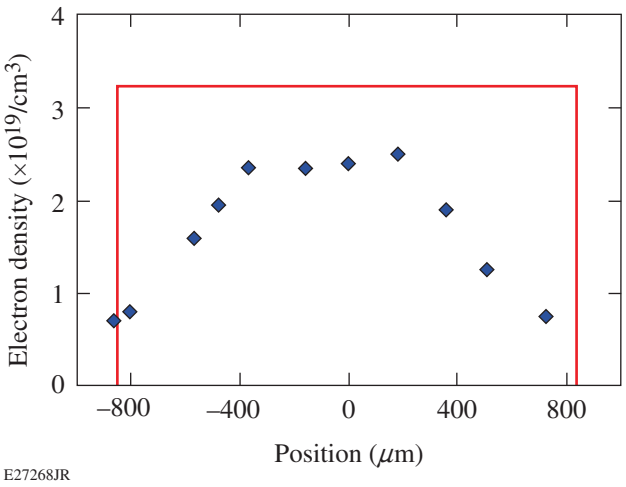

Figure 154.35
Electron density versus position in the gas-jet plasma at 400 ps. A constant density is measured in the central portion of the plasma volume. The outer part of the plasma density drops off linearly because of a rarefaction wave. The analytic model (shown in red) predicts a peak density ~30% higher than the measured peak density. The lower-density fringes of the plasma exceed the predicted bounds of the neutral gas as a result of hydrodynamic expansion in the plasma.

Summary

A gas-jet system has been activated on the OMEGA Laser System. Design considerations for supersonic nozzles and other target parameters have been analyzed in depth using an analytic model for compressible gas flow. The OMEGA gas-jet system has been characterized using a Mach–Zehnder interferometer to study neutral density and timing characteristics. The gas-jet plasma has been characterized using Thomson scattering with the OMEGA laser to measure plasma density across a plasma volume heated by 11 UV beams. In each of these studies the gas jet was found to have excellent characteristics, which will provide a flexible platform for a wide variety of experiments.

ACKNOWLEDGMENT

This material is based upon work supported by the Department of Energy National Nuclear Security Administration under Award Number DE-NA0001944, the University of Rochester, and the New York State Energy Research and Development Authority.

REFERENCES

1. D. Turnbull, C. Goyon, G. E. Kemp, B. B. Pollock, D. Mariscal, L. Divol, J. S. Ross, S. Patankar, J. D. Moody, and P. Michel, Phys. Rev. Lett. **118**, 015001 (2017).
2. A. Döpp *et al*., Rev. Sci. Instrum. **87**, 073505 (2016).
3. D. H. Kalantar *et al*., Phys. Plasma **2**, 3161 (1995).
4. T. R. Boehly, R. S. Craxton, T. H. Hinterman, J. H. Kelly, T. J. Kessler, S. A. Kumpan, S. A. Letzring, R. L. McCrory, S. F. B. Morse, W. Seka, S. Skupsky, J. M. Soures, and C. P. Verdon, Rev. Sci. Instrum. **66**, 508 (1995).
5. M. Krishnan *et al*., Phys. Rev. Spec. Top., Accel. Beams **14**, 033502 (2011).
6. J. Katz, R. Boni, C. Sorce, R. Follett, M. J. Shoup III, and D. H. Froula, Rev. Sci. Instrum. **83**, 10E349 (2012).
7. S. Semushin and V. Malka, Rev. Sci. Instrum. **72**, 2961 (2001).
8. K. Schmid and L. Veisz, Rev. Sci. Instrum. **83**, 053304 (2012).
9. D. H. Froula *et al*., *Plasma Scattering of Electromagnetic Radiation: Theory and Measurement Techniques*, 2nd ed. (Academic Press, Amsterdam, 2011).
10. A. J. Mackinnon, S. Shiromizu, G. Antonini, J. Auerbach, K. Haney, D. H. Froula, J. Moody, G. Gregori, C. Constantin, C. Sorce, L. Divol, R. L. Griffith, S. Glenzer, J. Satariano, P. K. Whitman, S. N. Locke, E. L. Miller, R. Huff, K. Thorp, W. Armstrong, W. Bahr, W. Seka, G. Pien, J. Mathers, S. Morse, S. Loucks, and S. Stagnitto, Rev. Sci. Instrum. **75**, 3906 (2004).
11. R. K. Follett, J. A. Delettrez, D. H. Edgell, R. J. Henchen, J. Katz, J. F. Myatt, and D. H. Froula, Rev. Sci. Instrum. **87**, 11E401 (2016).